Electronic Supplementary Material (ESI) for CrystEngComm.

Electronic Supplementary Information

Multifunctionality of weak ferromagnetic porphyrin-based MOF: selective adsorption in liquid and gas phase.

Eder Amayuelas,*[,a] Paul Iacomi,*[,b] Arkaitz Fidalgo-Marijuan,[c] Begoña Bazán,[a,c] Miren Karmele Urtiaga,[a] Gotzone Barandika,[c,d] Luis Lezama,[d] Philip Llewellyn[b] and María Isabel Arriortua.[a,c]

[a]*Departament of Mineralogy and Petrology, University of the Basque Country, Sarriena, 48940, Leioa, Spain.*
[b]*Aix-Marseille University, CNRS, MADIREL UMR 7246, 13397 Marseille, France.*
[c]*BCMaterials, Basque Center for Materials, Applications and Nanostructures, Bld. Martina Casiano, 3rd Floor, UPV/EHU Science Park, 48940, Leioa, Spain.*[de]*Department of Organic Chemistry II, University of the Basque Country, Sarriena, 48940, Leioa, Spain.*
[d]*Departament of Inorganic Chemistry, University of the Basque Country, Sarriena , 48940, Leioa,Spain.*

Synthesis of $[Ni_5(H2TCPP)_2O(H_2O)_4]\cdot nS$ (1)

Meso-tetra(4-carboxyphenyl)porphyrin (7.9 mg, 0.01 mmol), nickel(II) nitrate hexahydrate >98.5% (29.7 mg, 0.1 mmol) and modulating agent 1,2,4,5-benzenetetracarboxylic acid 96% (15.7 mg, 0.06 mmol) were dissolved in DMF (5 mL) in a small capped vial, sonicated to ensure homogeneity and heated to 100 °C for 72 h, yielding diffraction quality prismatic dark red crystals. This freshly synthesized product was washed with acetone several times before single crystal X-ray diffraction experiments.

Thermal stability of 1

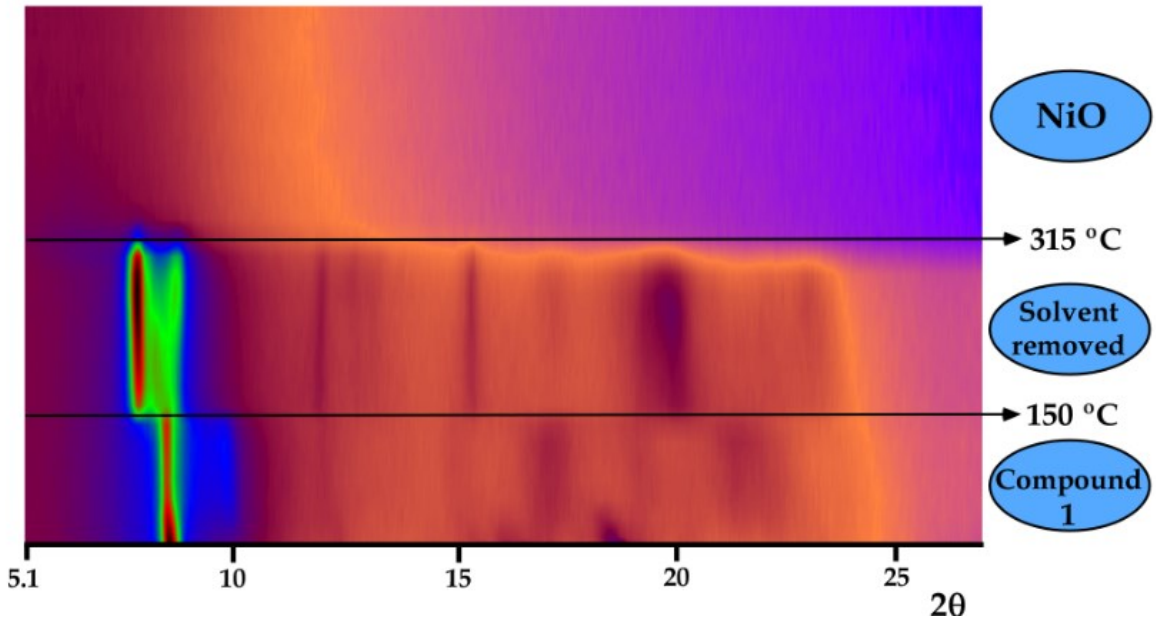

Figure S1. Zenithal view of the thermodiffractometry for compound **1**. Black lines mark the temperature in which main peaks shift (150 C) due to solvent removal and in which compound **1** totally degrades (315 C).

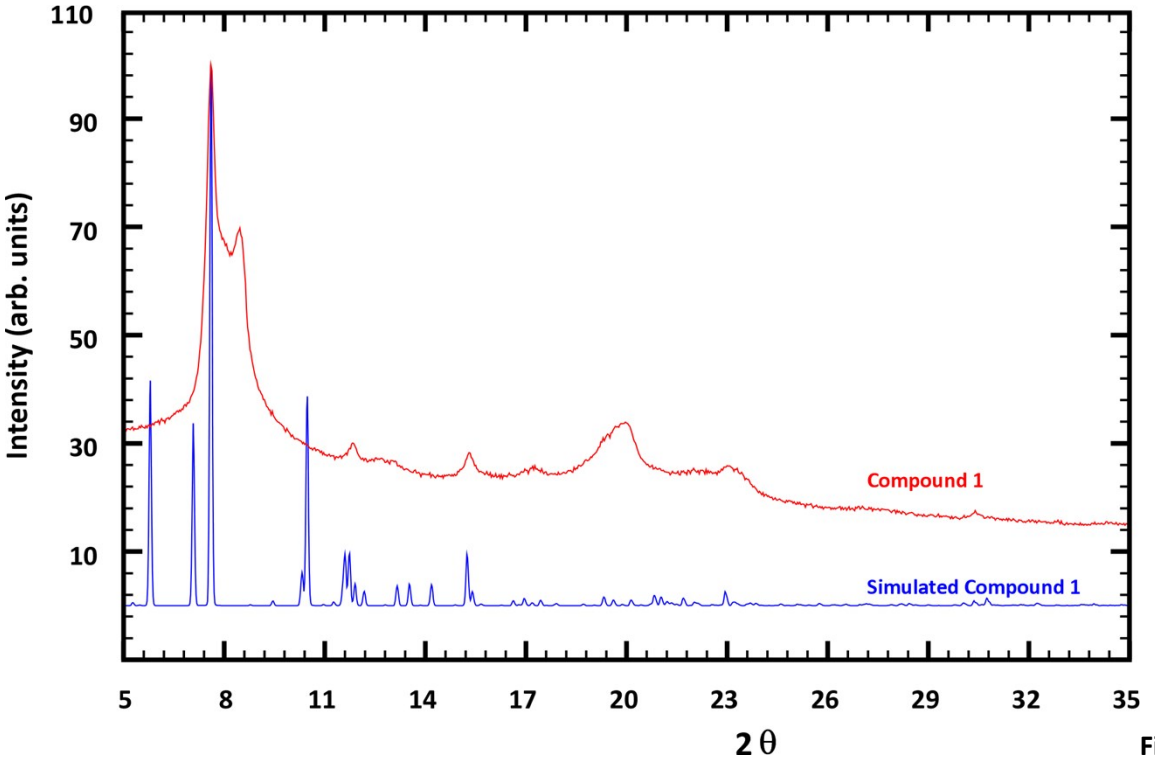

Figure S2.

Experimental and simulated powder X-ray diffraction pattern of compound **1**.

Magnetic properties of 1

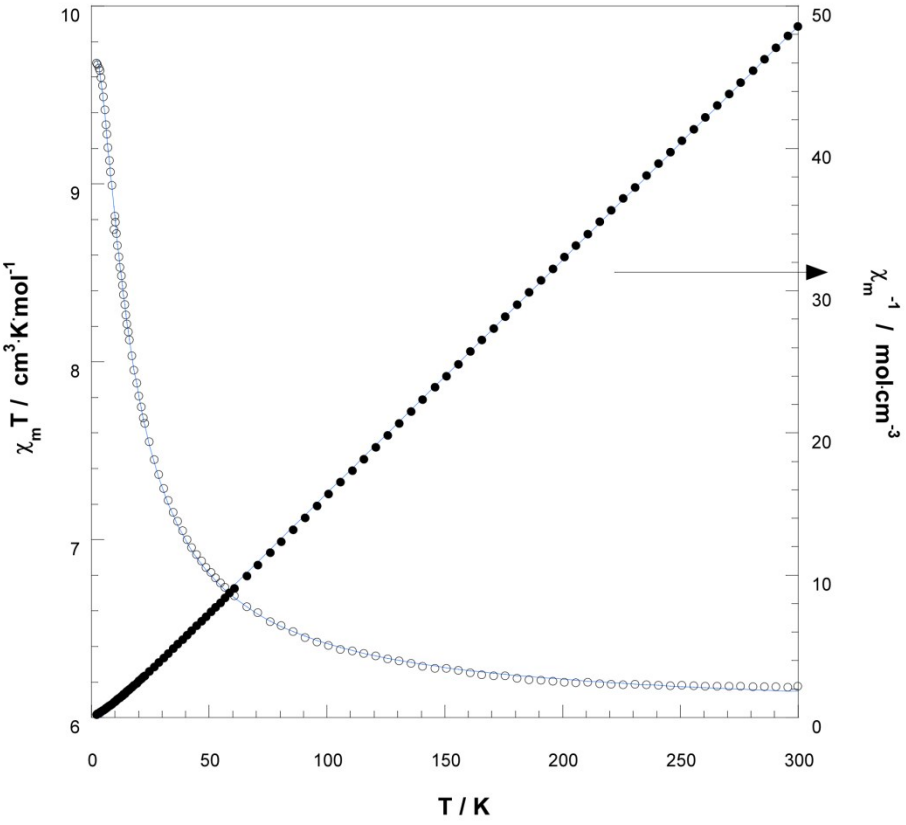

Figure S3. Thermal variation of the χ_m^{-1} and $\chi_m T$ parameters for compound **1**. Solid lines represent best model fit.

Dye adsorption

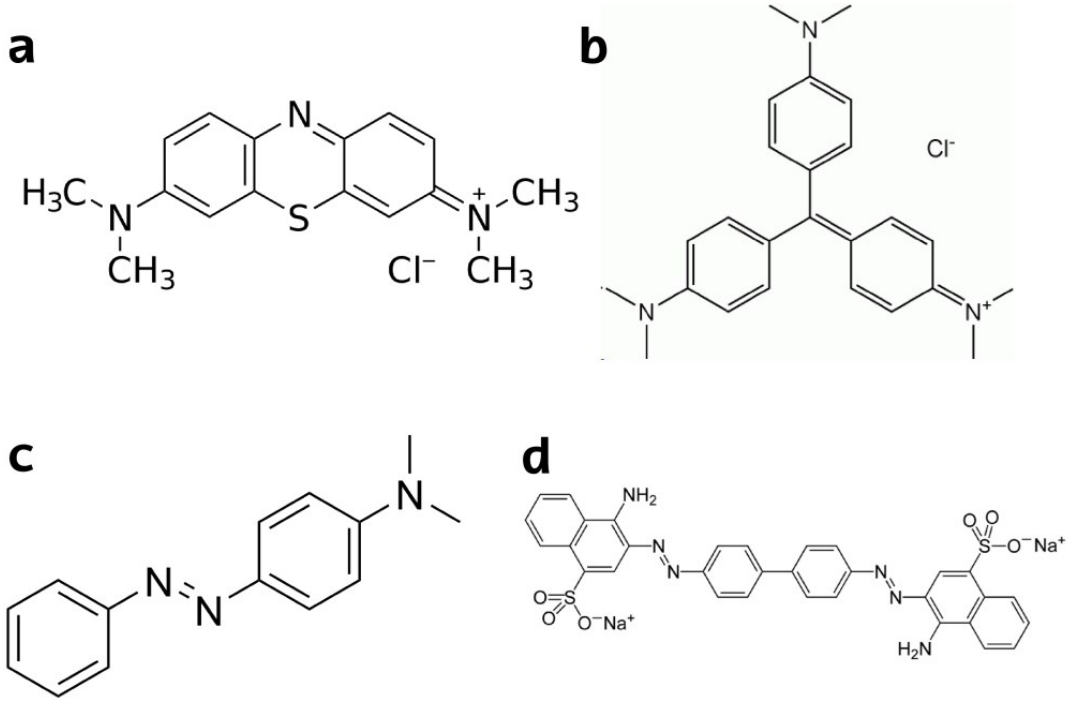

Figure S4. Molecular structure of dyes used in adsorption tests. (a) methylene blue (**MB**), (b) crystal violet (**CV**), (c) dimethyl yellow (**DY**) and (d) Congo red (**CR**).

Table S1. Molecular dimensions (Å) of dyes.

	MB	CR	DY	CV
***x* (width)**	4.59	5.38	4.5	4.47
***y* (height)**	8.01	7.9	6.0	12.97
***z* (length)**	14.75	25.1	13.1	13.74

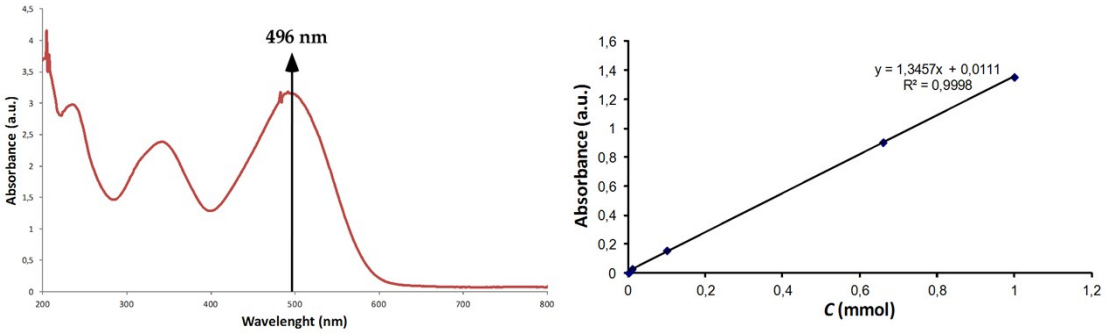

(a) (b)

Figure S5. (a) **CR** UV-Vis spectrum and (b) calibration line performed with solutions of different concentrations of **CR** ($1x10^{-4}$ M, $1x10^{-5}$ M, $1x10^{-6}$ M and $1x10^{-7}$ M). UV-Vis measurements for **CR** were performed at 496 nm.

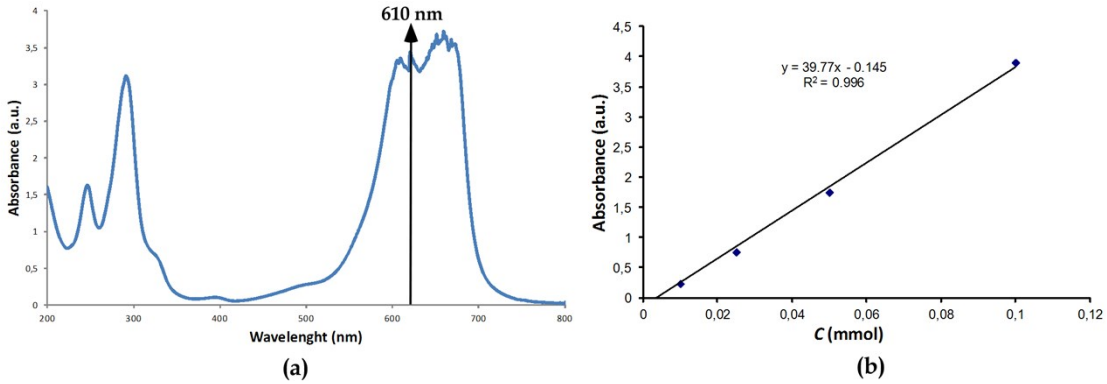

Figure S6. (a) **MB** UV-Vis spectrum and (b) calibration line performed with solutions of different concentrations of **MB** ($1x10^{-4}$ M, $1x10^{-5}$ M, $1x10^{-6}$ M and $1x10^{-7}$ M). UV-Vis test for **MB** were measured at 610 nm.

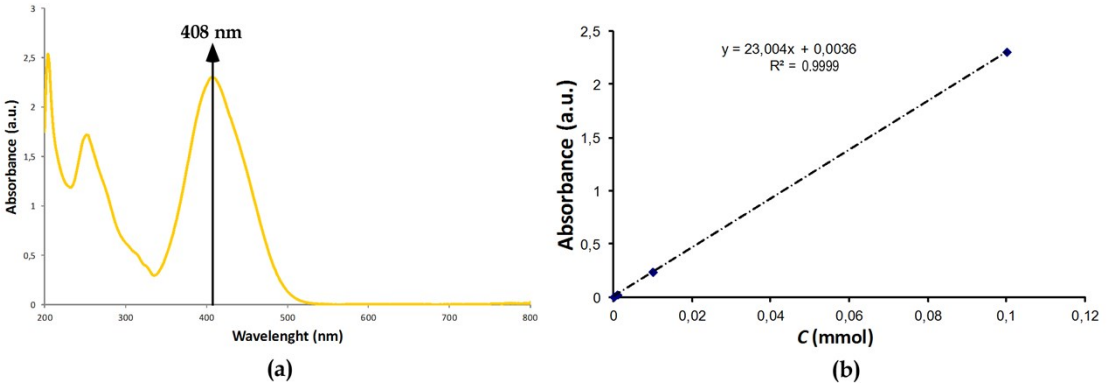

Figure S7. (a) **DY** UV-Vis spectrum and (b) calibration line performed with solutions of different concentrations of **DY** ($1x10^{-4}$ M, $1x10^{-5}$ M, $1x10^{-6}$ M and $1x10^{-7}$ M). UV-Vis test for **DY** were measured at 408 nm.

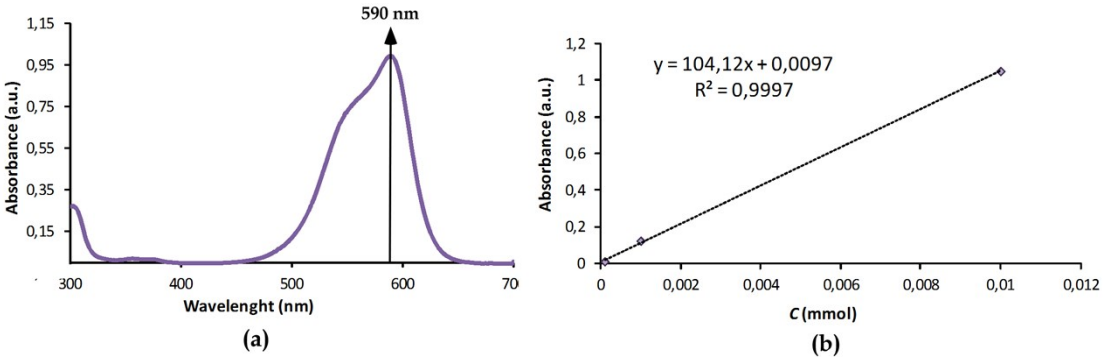

Figure S8. (a) **CV** UV-Vis spectrum and (b) calibration line performed with solutions of different concentrations of **CV** ($1x10^{-4}$ M, $1x10^{-5}$ M, $1x10^{-6}$ M and $1x10^{-7}$ M). UV-Vis test for **CV** were measured at 408 nm.

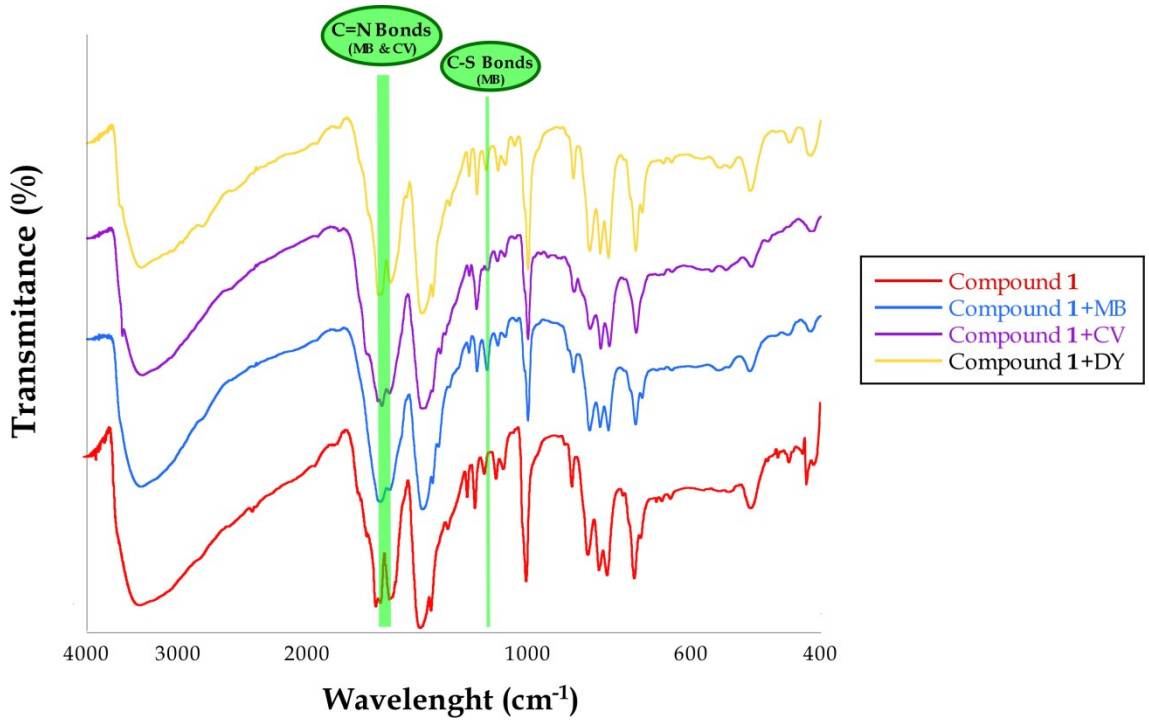

Figure S9. IR of compound **1** and samples loaded with **MB**, **CR** and **DY.**

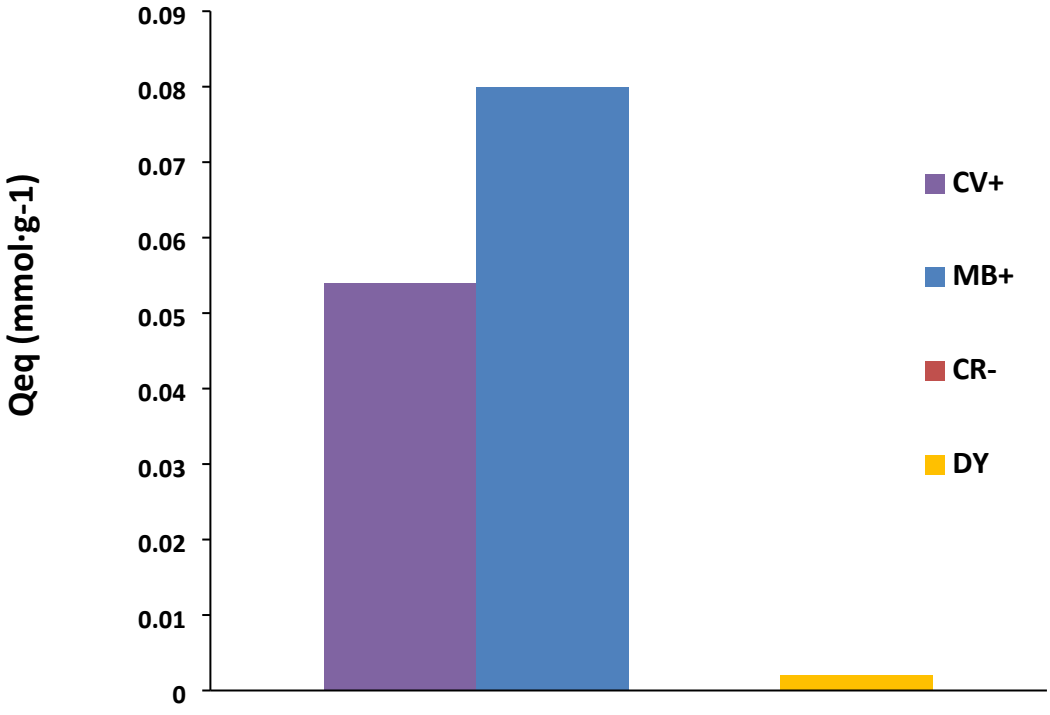

Figure S10. Adsorbed amount of each dye by compound 1 after 15 days.

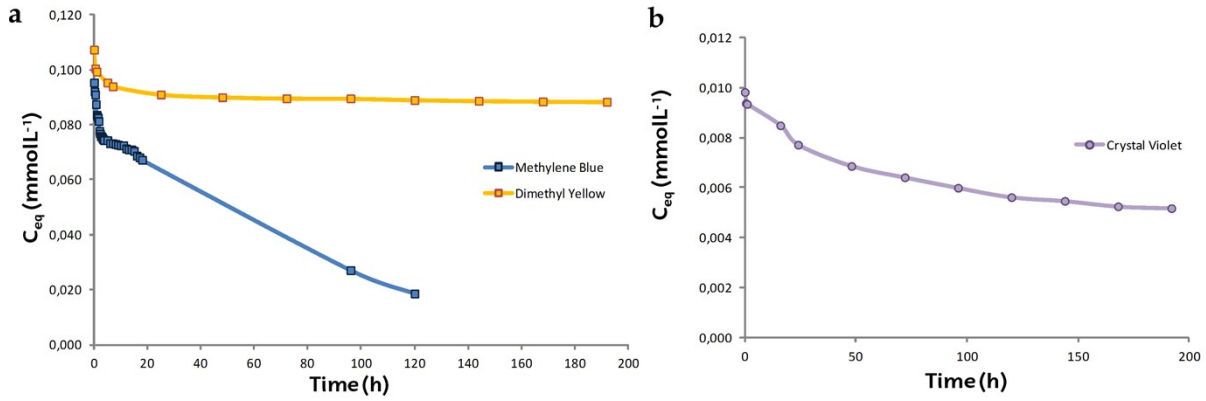

Figure S11. Concentration changes for (a) **MB** (blue), **DY** (yellow) and for (b) **CV** (purple).

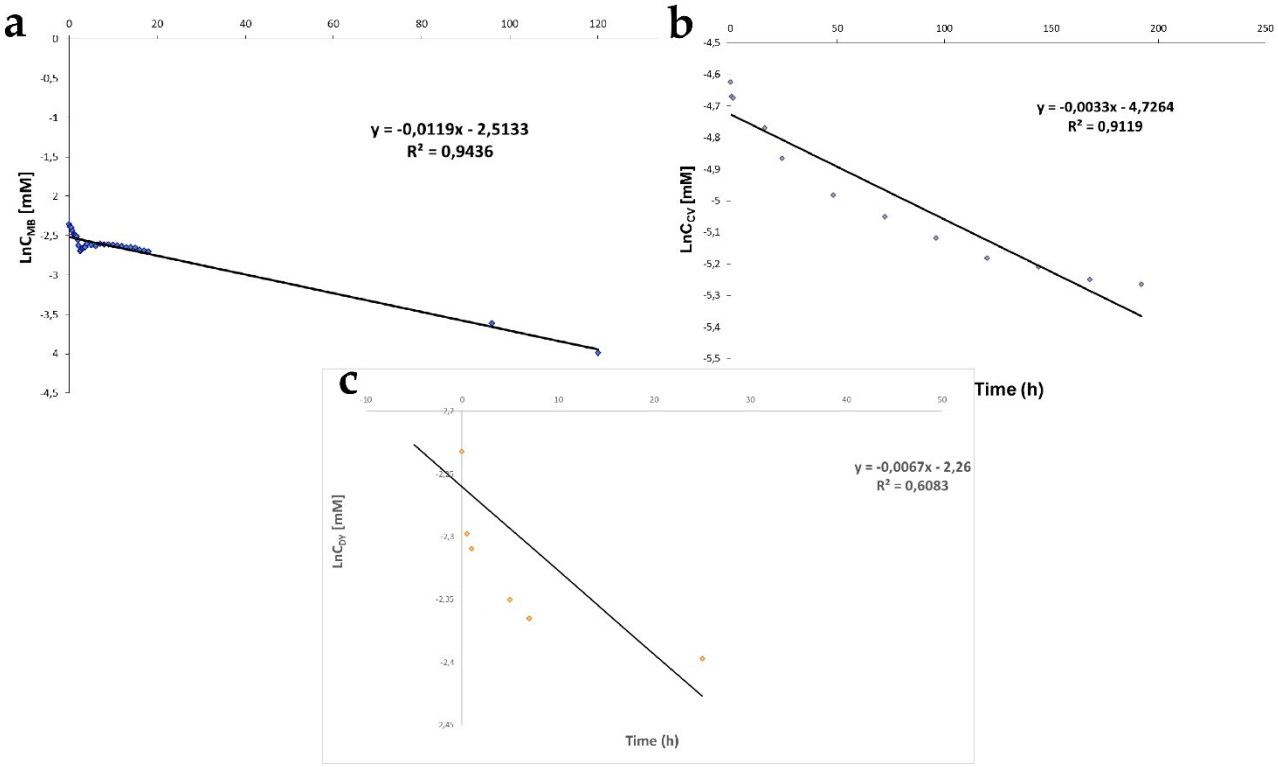

Figure S12. First order kinetics adjustment for (a) **MB**, (b) **CV** and (c) **DY**.

N2 physisorption at 77 K

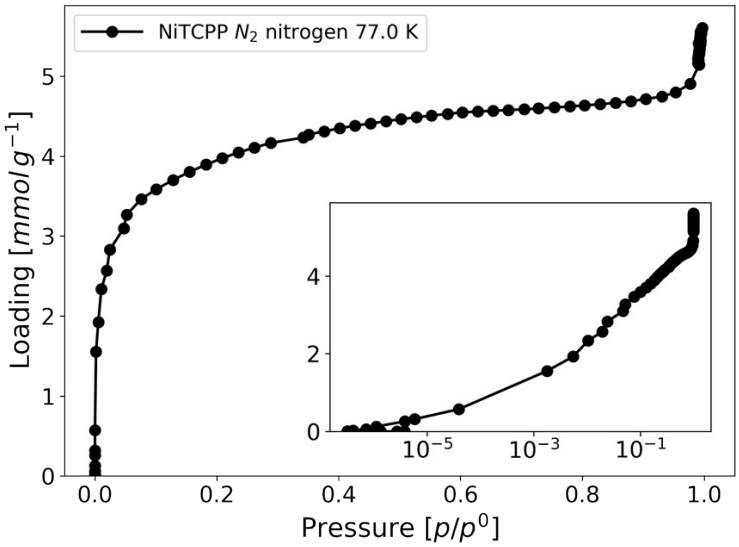

Figure S13. N_2 adsorption isotherm at 77 K for compound **1**.

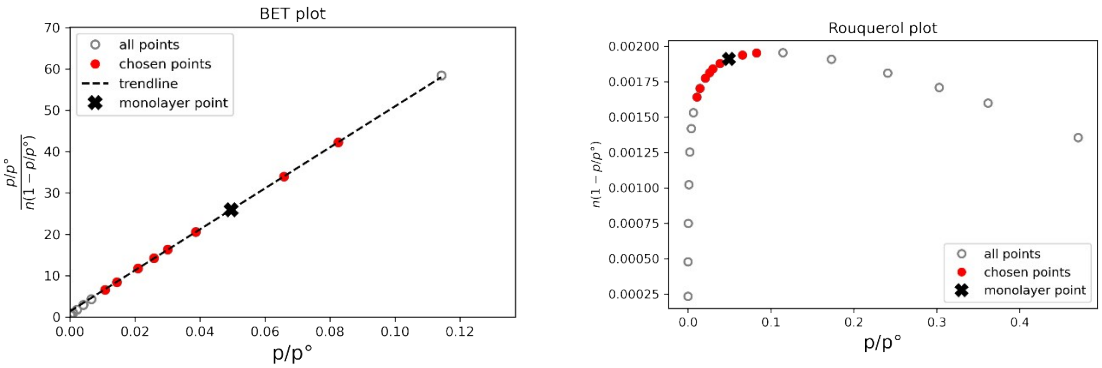

Figure S14. BET plot (left) and Rouquerol plot (right) for the nitrogen adsorption isotherm above. Computed BET surface area is 388 m^2g^{-1}.

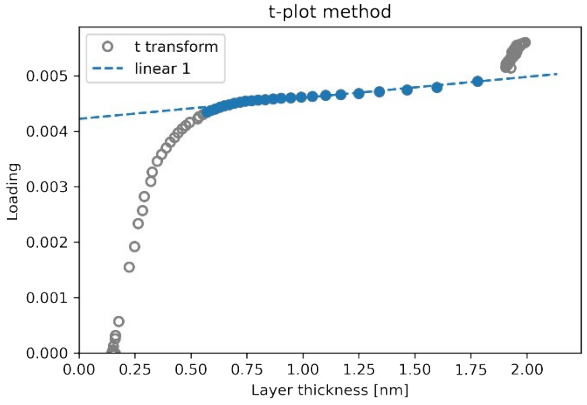

Figure S15. t-plot of the nitrogen adsorption on **1**. Computed micropore volume is 0.15 cm^3g^{-1}.

Probe physisorption at 303 K

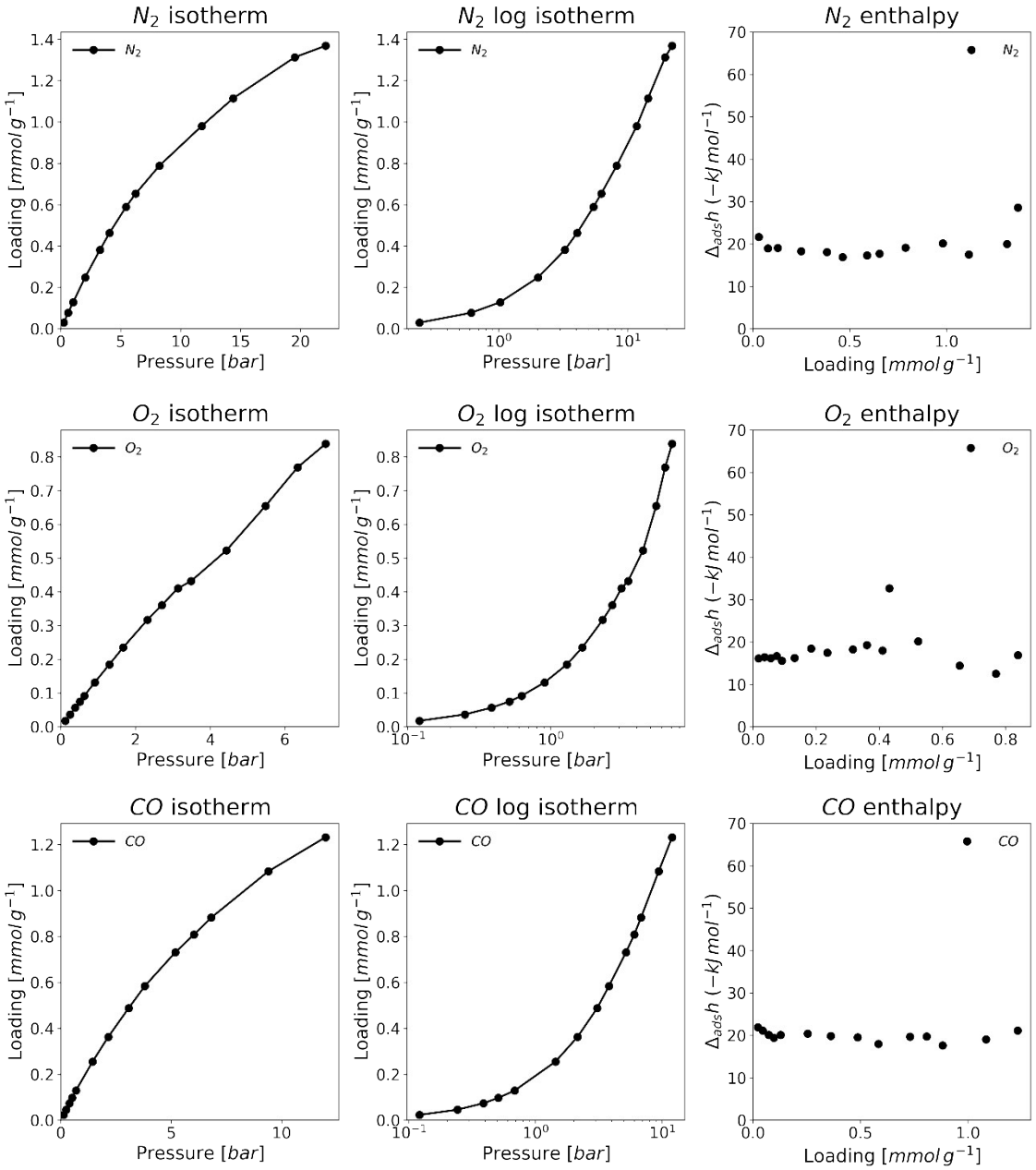

Figure S16. Gas adsorption isotherms and differential enthalpy for N_2, O_2 and CO at 303 K.

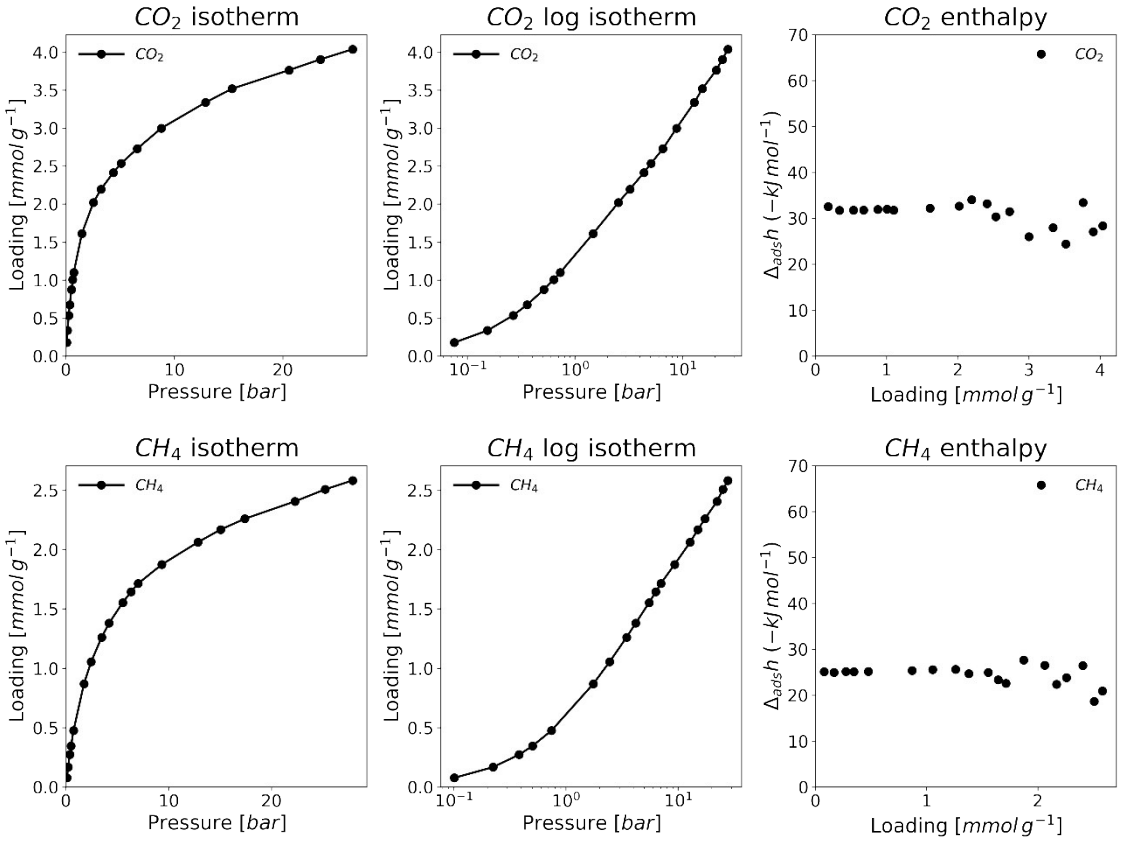

Figure S17. Gas adsorption isotherms and differential enthalpy for CO_2 and CH_4 at 303 K.

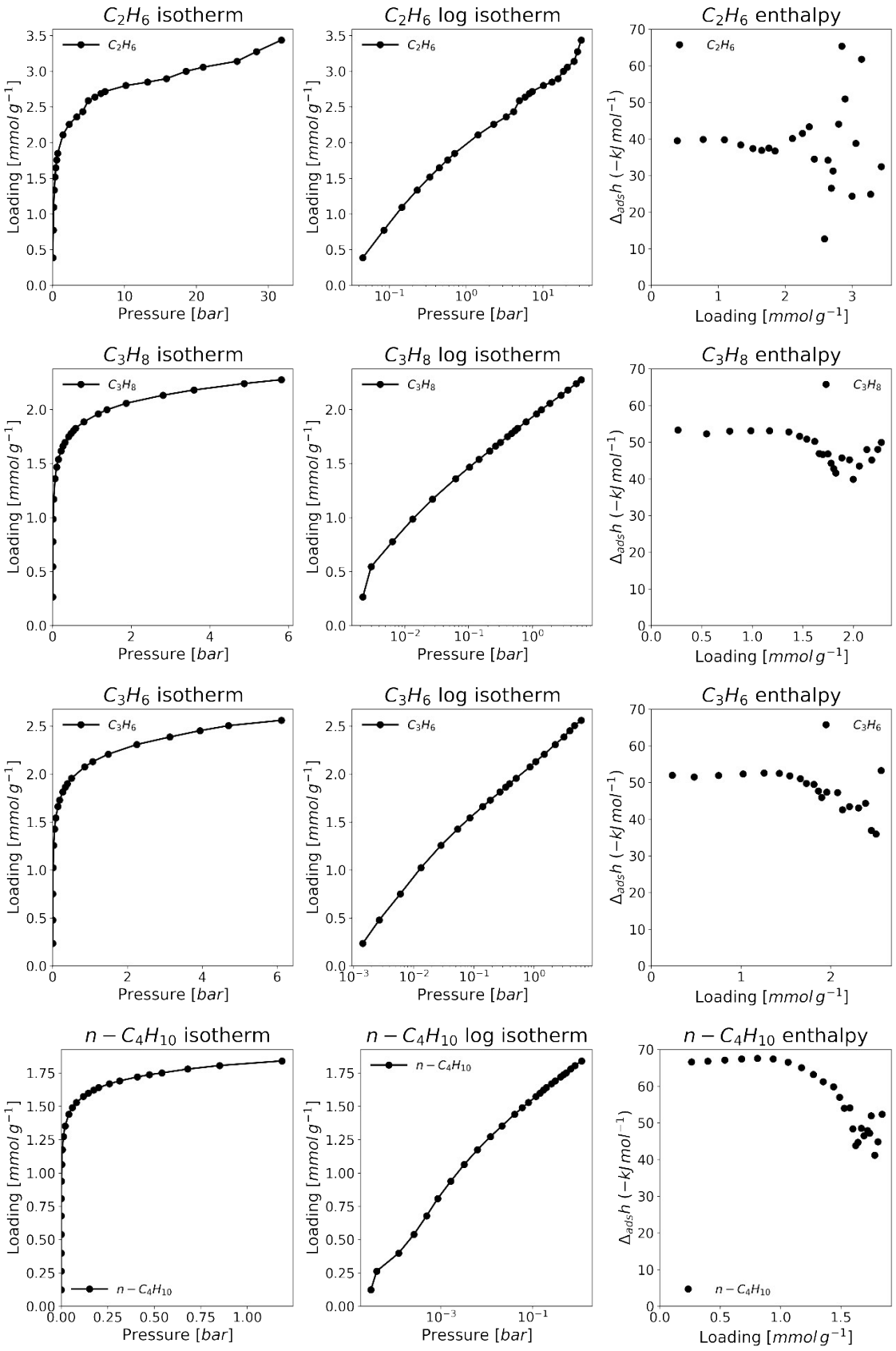

Figure S18. Gas adsorption isotherms and differential enthalpy for C_2H_6, C_3H_8, C_3H_6, C_4H_{10} at 303 K.

IAST binary sorption predictions

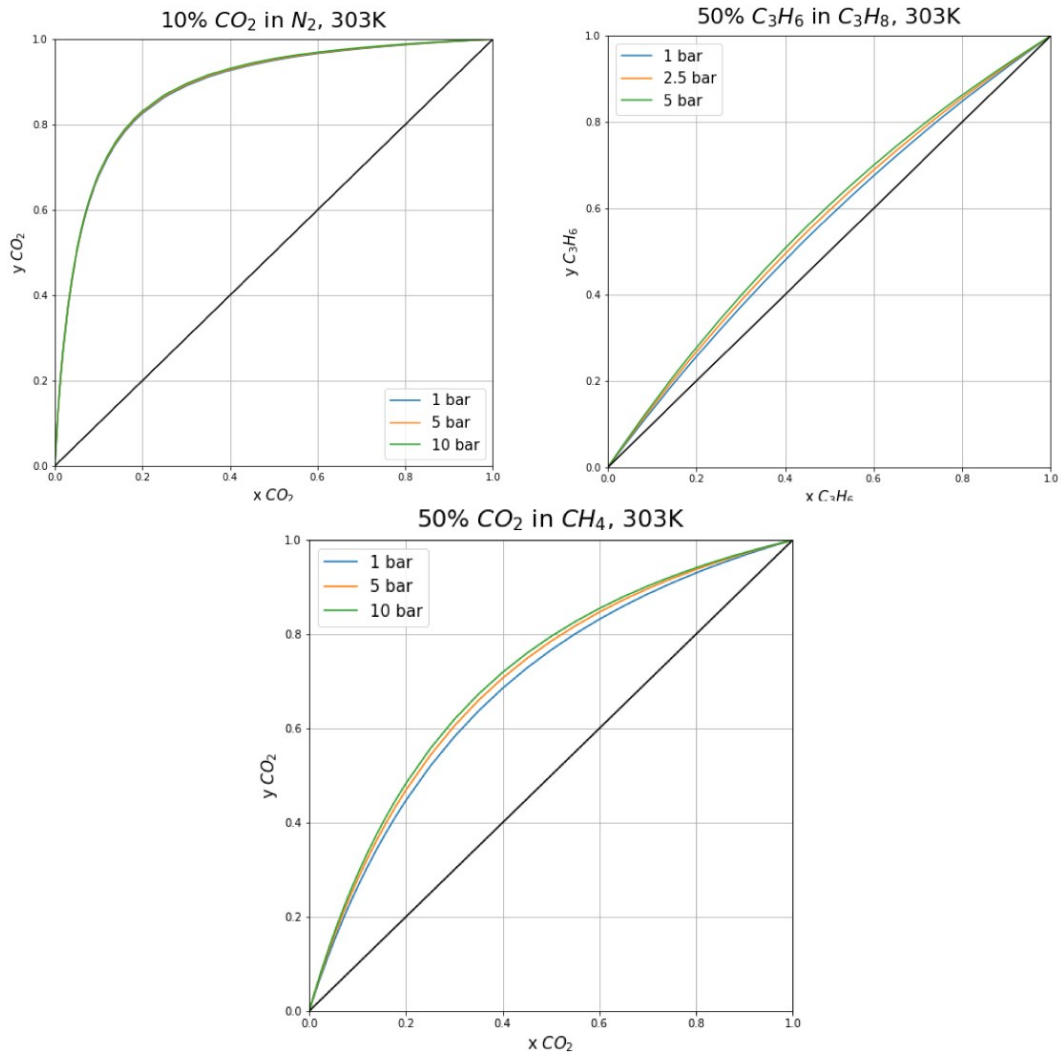

Figure S19. Selectivity curves obtained through IAST simulations. Curves overlap if the selectivity does not change with pressure.